TOTAL AND BOUNDARY PRECIPITABLE WATER RETRIEVAL FROM AMSU

Wenjian Zhang[*], W. P. Menzel, Jun Li, W. Wolf, H. M. Woolf, P. Van Delst, T.H. Achtor
Cooperative Institute for Meteorological Satellite Studies
Space Science and Engineering Center, University of Wisconsin-Madison
Madison, Wisconsin 53706, USA

1. INTRODUCTION

Water vapor, the most significant greenhouse gas, plays a fundamental role in the energy and water cycle processes that determine weather and climate. Water vapor is especially important in the troposphere because of its role in exerting great control over the dynamics, thermodynamics and the chemistry of the atmosphere. However, water vapor is also one of the most variable parameters of the atmosphere. The accurate determination of the Total Precipitable Water (TPW) and its horizontal distribution in the atmosphere is one of the most challenging tasks.

One of the key features of the vertical distribution of water vapor is that it decreases exponentially with height. About 60% of the TPW in the atmosphere are concentrated between sea level and 850 hPa (boundary layer); Less than 10% can be found above 500 hPa. Therefore, determination of boundary layer precipitable water is important for weather forecasting and climate change research. It is well known that the global distribution of water vapor can only be obtained by radiative measurements from satellite platforms.

Three factors control the absorption of the energy reaching the satellite sensors (P. K. Rao, et. al, 1990). The first two factors, the degree of absorption at each wavelength and the distribution of the absorbing gas within the atmosphere, are numerically described by a calculated weighting function. The third factor, the temperature along the radiation path, is expressed as the Planck Function. An important difference between the problems posed by the retrieval of the temperature profile and those posed by the water vapor profile retrievals should be mentioned (F. T. Ulaby 1982). Whereas the temperature profile has a basically stable structure and a relative variability about the mean profile $\langle T(z) \rangle$ on the order of 0.2, the water vapor density may exhibit large variations as a function of both space and time. For a fixed location, the TPW can vary by a factor of 30 during a given year.

There are many algorithms for retrieving moisture profiles and TPW based on infrared sensors. For moisture profile retrieval, the important channels are the water vapor absorption channels. However, window channels are predominantly used for TPW retrieval. With the launch of the NOAA-15 satellite on 13 May 1998, the

* Visiting scientist from National Satellite Meteorological Center (NSMC), Beijing, CHINA

Advance Microwave Sounding Unit (AMSU) adds a new sounding capability. The AMSU-A is a cross track, line-scanned instrument designed to measure scene radiance in 15 discrete frequency channels. Each stepped-scan line has thirty contiguous scene observations. At each channel, the antenna beamwidth is a constant 3.3 degrees, which translates to a 50 km diameter cell at nadir, and the 50 degree scanning angle on each side of the sub-satellite path translates to a 2343 km swath width from the 833 km nominal orbital altitude. There are 4 window channels among the 15 AMSU-A channels and some near window channels, which can be used for retrieving surface parameters, precipitation, and TPW from this satellite borne microwave instrument.

2. PHYSICAL BASIS

One of the difficulties for retrieving the water vapor is that it is very hard to measure the lower troposphere (boundary layer) moisture over surfaces with high emissivites. To illustrate this, assume an isothermal atmosphere from Zs to Z with an average temperature T. The radiance observed by a zenith-viewing satellite sensor at a window channel is given by (assuming the surface emissivity is equal to one),

$$R(v) = R_s(v)\tau_s(v) + B(v,T)[1-\tau_s(v)]\cdots\cdots(1),$$

where $R(v)$ is the satellite radiance, $\tau_s(v)$ the water vapor transmittance, $R_s(v)$ the surface radiance and $B(v,T)$ the Plank function. If $R_s(v)$ is not equal to $B(v,T)$, then we have

$$\tau_s(v) = \frac{R(v)-B(v,T)}{R_s(v)-B(v,T)}\cdots\cdots(2)$$

However, if $R_s(v)=B(v,T)$, one cannot obtain $\tau_s(v)$ from equation (2) (Zeng Qingcun, 1974). Therefore the measurement of $R(v)$ cannot provide any information about the water vapor distribution. This is true for IR sensors while sensing the boundary layer moisture over both land and oceans. This is also true for microwave sensors over dry land with emissivities larger than 0.9. However, for microwave remote sensing over oceans, the surface is a radiometrically cold background. Neglecting the surface reflectance (usually this term is very small compared with other terms), the equation for microwave remote sensing in a window channel can be obtained in brightness temperature form:

$$\tau_s(v) = \frac{T_B(v)-T}{T_s\varepsilon_s(v)-T}\cdots\cdots(3),$$

where T_B is the measured brightness temperature, T_s is the surface-skin temperature, and ε_s is the surface emissivity. From this equation, one can see that if the surface emissivity is close to unit, the situation is the same as IR sensors. However, if ε_s is much less than 1, for example the sea surface with the microwave

Figure 1. AMSU-A Water Vapor Weighting Functions

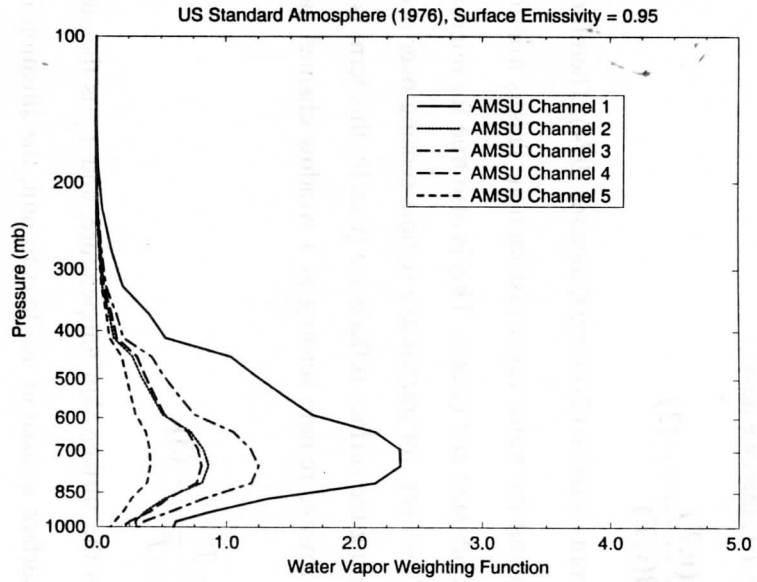

Figure 2. AMSU-A Water Vapor Weighting Function

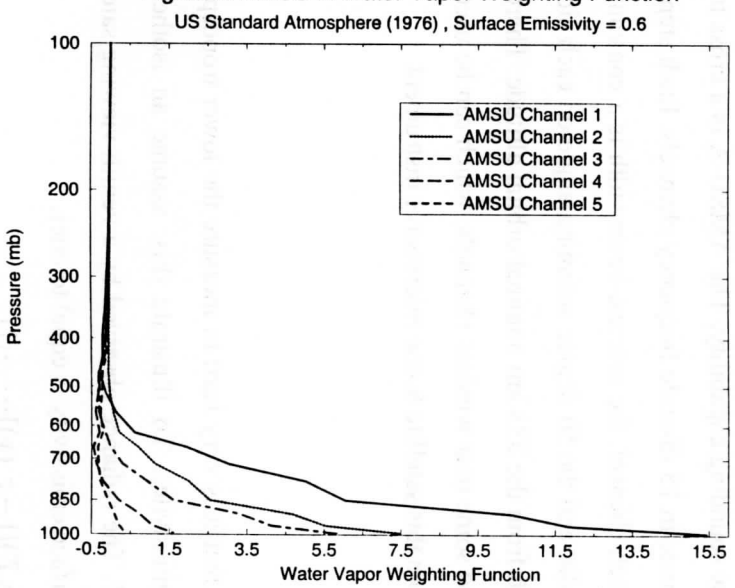

Figure 3. Simulation of TPW vs. Brightness Temperature of AMSU ch. 1 and 2

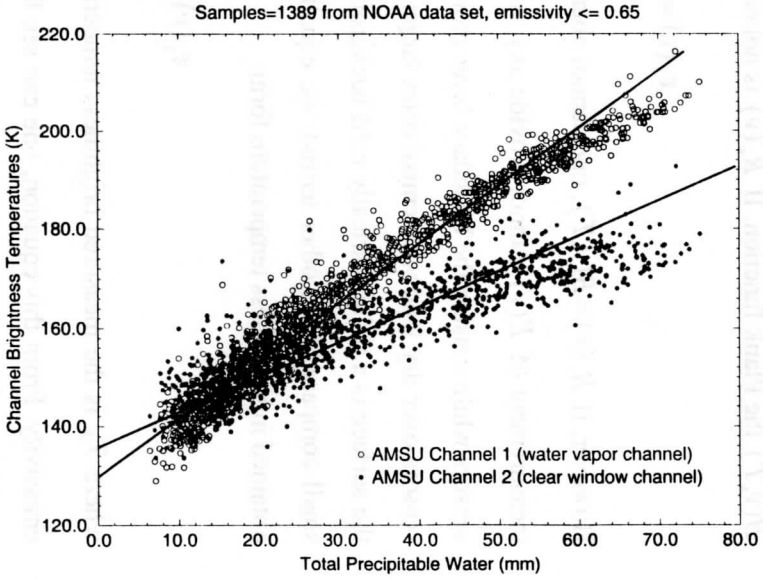

Figure 4. Simulation of AMSU 1 and 2 BT difference versus TPW

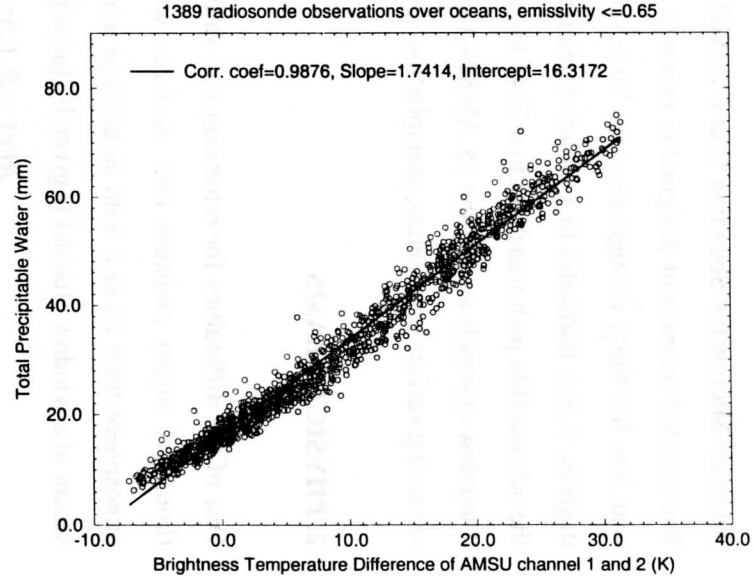

emissivity of 0.5-0.6, then the lower level water vapor information can be obtained by microwave observations, even under the conditions of $T_s \approx T$.

3. WATER VAPOR WEIGHTING FUNCTIONS AND SIMULATIONS

For more detailed understanding of the physics of retrieving the total precipitable water by AMSU-A, we can examine the AMSU water vapor component weighting functions (water vapor is expressed as the logarithm of the water vapor mixing ratio, i.e. $\frac{\partial \ln q}{\partial p}$, Jun Li, et al., 1994)

$$W_q = \{(T_s - T_a)\varepsilon_s \tau_s \beta_s - 2(1-\varepsilon_s)\int_0^{p_s} \beta\tau^* \frac{\partial T}{\partial p} dp\} \frac{\partial \ln \tau_w}{\partial p} \cdots\cdots (4)$$

where T_s is the surface skin temperature, T_a is the surface air temperature, $\beta = \frac{\partial B / \partial T}{\partial R / \partial T_B}$, ε_s is the surface emissivity, $\tau^* = \tau_s^2 / \tau$, etc. (the solar reflectivity is ignored).

Based upon this equation, the water vapor component weighting functions of AMSU can be drawn under different surface emissivity assumptions. Figure 1 is the AMSU-A water vapor weighting functions for channel 1-5 with a surface emissivity of 0.9. This is corresponds to the very dry land surface conditions for AMSU-A window channels. From these water vapor weighting functions, it can be seen that although AMSU-A channels 1-3 are window channels, however, their weighting function peaks are not at the surface, but near 700 mb. This is also true for the infrared sensors trying to sense the lower level water vapor above all surface types. From this information we can conclude that the satellite sensors (both infrared and microwave) can mainly sense the middle and upper level moisture, but they are not suitable for sensing the water vapor in the lower troposphere over dry land surfaces.

Figure 2 also shows the AMSU-A channel 1-5 weighting function but with a surface emissivity of 0.6. It clearly indicates that the weighting functions peak near the surface, which reinforces the above discussions and means that AMSU window channels are suitable for sensing the lower troposphere moisture over oceans. Among these channels, AMSU-A channel 1, centered at 23.8 MHz near the water vapor absorption line, is the most sensitive channel for lower troposphere water vapor retrieval. This is the physical basis for retrieving boundary precipitable water over oceans by the AMSU-A instrument.

4. ALGORITHM DEVELOPMENT

4.1 Theoretical analysis

For a non-scattering atmosphere in local thermodynamic equilibrium, the equation for radiative transfer provides the following integral solution for a satellite borne microwave sensor:

$$T_B = T_s \varepsilon_s \tau_s - \int_0^{p_s} T(p) \frac{\partial \tau}{\partial p} dp - (1-\varepsilon_s)\tau_s \int_0^{p_s} T(p) \frac{\partial \tau^*}{\partial p} dp \cdots\cdots (5)$$

where T_B is the brightness temperature measured by the sensor and $T(p)$ is the thermometric temperature of the atmosphere at pressure P. The other definitions are the same as in previous sections. The first term is also called the surface component, the second the direct radiation component, and the third reflectance component.

Considering the ocean surface roughness can also increase the brightness temperatures and therefore introduce a false signal. A reference channel is needed for eliminating the ocean roughness and the effects of the surface temperature variations. This reference channel should be less sensitive to the absorption by water vapor and other gases. Clearly, the AMSU-A channel 2 is the most preferred channel (it is also the cleanest channel among the AMSU-A channels with a total transmittance large than 0.9) as the reference channel.

Figure 3 shows the simulation results of the brightness temperatures of AMSU-A channel 1 and 2 versus TPW. In the simulation, a radon noise factor was added to the surface emissivity, allowing 10% surface emissivity variations around the mean emissivity value of 0.6 for ocean. The scattering of this figure reflects the uncertainties in surface emissivity and atmospheric water vapor variation. One can see that the brightness temperatures of AMSU-A channel 1 increase more rapidly than those of AMSU-A channel 2 with the increase of TPW. Figure 4 depicts the brightness temperature differences of AMSU-A channel 1 and 2 versus TPW. By using the brightness temperature difference, most of the surface uncertainties are eliminated and a good linear relationship between TPW and brightness temperature difference is well established.

Assuming two window channels are spectrally so close that the surface emissivity differences can be ignored, the brightness temperature of the specific channel with respect to a reference channel can be expressed as:

$$\Delta T_B = T_B(i) - T_B(f) = T_s \varepsilon_s [\tau_s(i) - \tau_s(f)] + (1-\varepsilon_s)\tau_s [T_d(i) - T_d(f)] + [T_u(i) - T_u(f)] \cdots\cdots (6),$$

where the "(f)" term represents the reference channel and T_d and T_u are the brightness temperature of downward and upward components. In order to simplify the equation and establish the algorithm, it is necessary to examine quantitatively the different terms and the differences between the two channels for each term, as indicated in Table 1.

Table 1. Brightness temperature components and differences of AMSU channel 1 and 2

	Channel BT(k)	Surface term(k)	Reflectance (k)	Direct (k)
Ch1(nadir)	178.0	147.0	9.0	22.0
Ch2(nadir)	171.0	151.0	6.0	14.0
Ch1-Ch2(nadir)	7.0	-4.0	3.0	8.0
Ch1(limb)	186.0	140.0	13.0	33.0
Ch2(limb)	176.0	147.0	9.0	20.0
Ch1-Ch2(limb)	10.0	-7.0	4.0	13.0
Limb-nadir diff.	3.0	-3.0	1.0	5.0

* The surface emissivity is assumed as 0.6 for this simulation, US standard atmospheric model (1976)

By analyzing Table 1, one can find that the reflectance term can be neglected, not only because this term itself is small, but also the difference between nadir and limb is also very small. Letting the $\overline{T}$ represent the mean temperature for the given window channels, the equation can be simplified as:

$$\Delta T_B = T_s \varepsilon_s [\tau_s(i) - \tau_s(f)] - \overline{T}[\tau_s(i) - \tau_s(f)] \cdots\cdots (7)$$

If U_t is the total precipitable water, then τ_s can be expressed as:

$$\tau_s(i) = \exp(-U_t \frac{\alpha(i)}{\mu}) \cdots\cdots (8),$$

where $\mu = \sec(\theta)$, θ is the satellite zenith angle, and α is a coefficient to be determined. Since the transmittance is relatively large in the atmospheric windows, equation (8) can be linearly approximated. Combining equations (7) and (8), the algorithm for retrieving total precipitable water can be obtained

$$U_t = \frac{\Delta T_B \mu}{(\overline{T} - \varepsilon_s T_s)[\alpha(i) - \alpha(f)]} \cdots\cdots (9)$$

Similarly, this is also valid for other low frequency AMSU channels, such as AMSU channel 3, while taking the AMSU channel 2 as the reference channel. In real data processing, we used the AMSU channels 1, 3, 4 and 5 brightness temperature difference versus the reference channel, as well as other ancillary information, such as satellite zenith angle, high level AMSU channel measurements, etc., in the equation as,

$$U_t = \sum_i \alpha_i X_i + \alpha_0 \cdots\cdots (10),$$

where $X_1 = T_{B1} - T_{B2}, X_2 = T_{B3} - T_{B2}$, $X_3 = T_{B4} - T_{B2}$, $X_4 = T_{B5} - T_{B2}$, $X_5 = T_{B6}$, $X_6 = T_{B7}$, $X_7 = T_{B8}$, $X_8 = T_{B12}(HIRS)$, $X_9 = \mu$, $X_{10} = abs(latitude)$, "abs" mean here the absolute value and α_i are coefficients to be determined.

This algorithm has several advantages. First, from equation (9) one can see that this algorithm is not dependent on surface temperature itself, but dependent on $\overline{T} - \varepsilon_s T_s$. This term is self-correlated and can be regarded as a constant. Secondly, this algorithm mainly uses lower frequency channels, which greatly minimize cloud scattering in most of the cases. The variations in the emissivity due to wind-generated roughness and foam are small compared to the changes in the transmittance due to water vapor.

4.2 Establishing the collocated data set

For generation of regression coefficients for the algorithm developed above, a global collocated (radiosonde observations with satellite measurements) data set is established. The criteria for selecting ATOVS measurements with radiosonde data for the collocated data set are based on the following:

- The collocation is based upon the IAPP retrieval bin (3*3 FOV array) and the nearest collocated radiosonde observations in both time and space;
- The absolute distance between the position (latitude and longitude) of the radiosonde and the ATOVS retrieval bin is less than 1.0 degree (the central FOV position among the 3*3 ATOVS FOV array is chosen representing the position of the ATOVS retrieval bin);
- The time difference between radiosonde and ATOVS measurements is less than ± 2 hours;
- The satellite zenith angle of the ATOVS measurement is less than 25.00 degree.

Based on these criteria, a global collocated data set has been established with more than 10,000 collocated files from November and December 1998. We used the November data set for algorithm development and the December data set for validation.

4.3 Generation of coefficients

Before generation of the coefficients, a cloud check for AMSU channels 1-4 has been applied to eliminate the cloud emission effects. Section 5 will discuss this in more detail. Another concern is that one must be very careful in selecting the collocated data set since most of the radiosonde stations are located on continental land. For ocean algorithm development, we have to select some ocean stations. However, even for some stations located on islands or near the coast, the land surface effects are still the major source for errors for the regression. By selecting the collocated data files located near the coast or at the island and then selecting the ocean FOV within the 9 FOVs, the ocean collocated data set is generated. Based on this data set, the regression coefficients for ocean and land are generated, respectively, by multi-linear regression. Applying these coefficients to the algorithm, the TPW and boundary precipitable water can be retrieved. The ASI is also used in the IAPP retrieval procedures.

Figure 5. AMSU Channel 1 and 2 BTs vs. Cloud Liquid Water Path

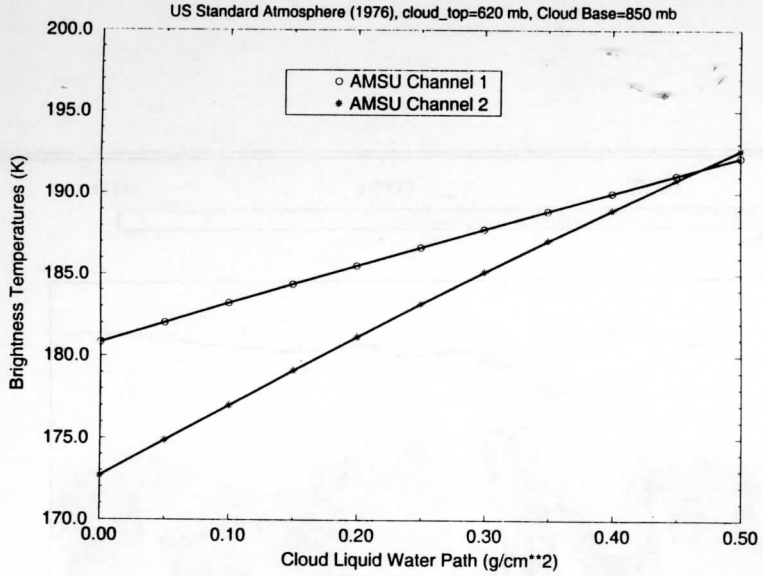

Figure 6. GOES 8 IR picture of Hurricane Mitch (12:45 UTC, Oct. 26, 1998). The AMSU scan line overlapped for AMSU BT response analysis (see figure 7)

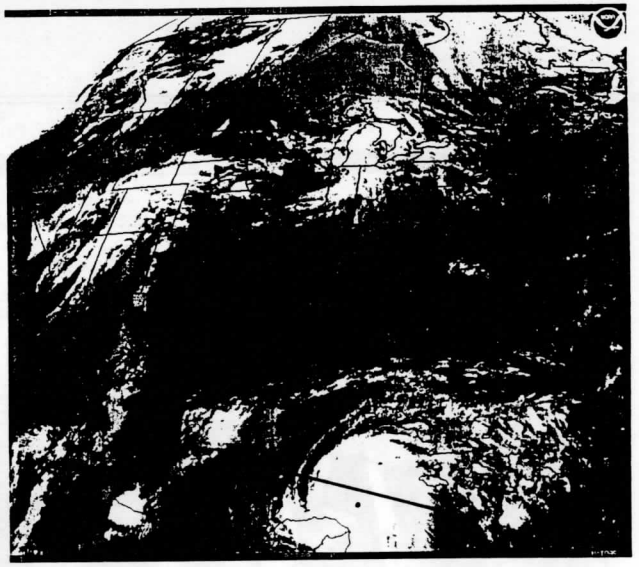

Figure 7. ATOVS Window channel BT response to Hurricane Mitch

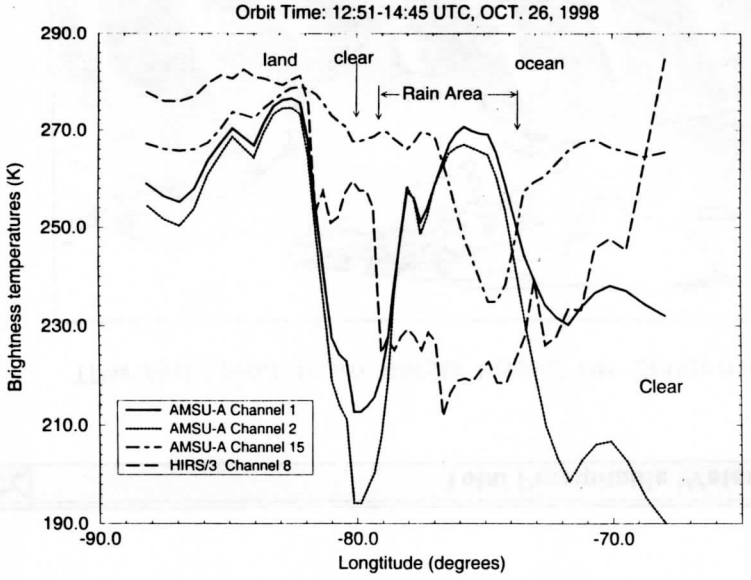

Figure 9. Scattering plot of Retrieved vs. Radiosonde TPW

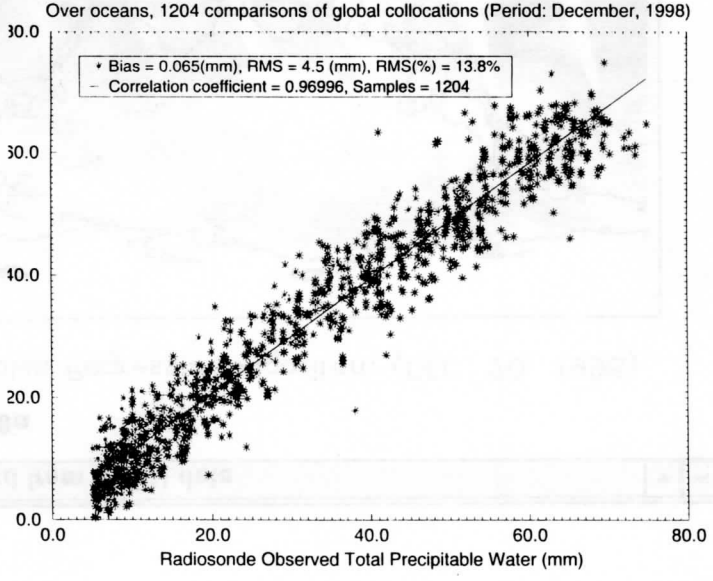

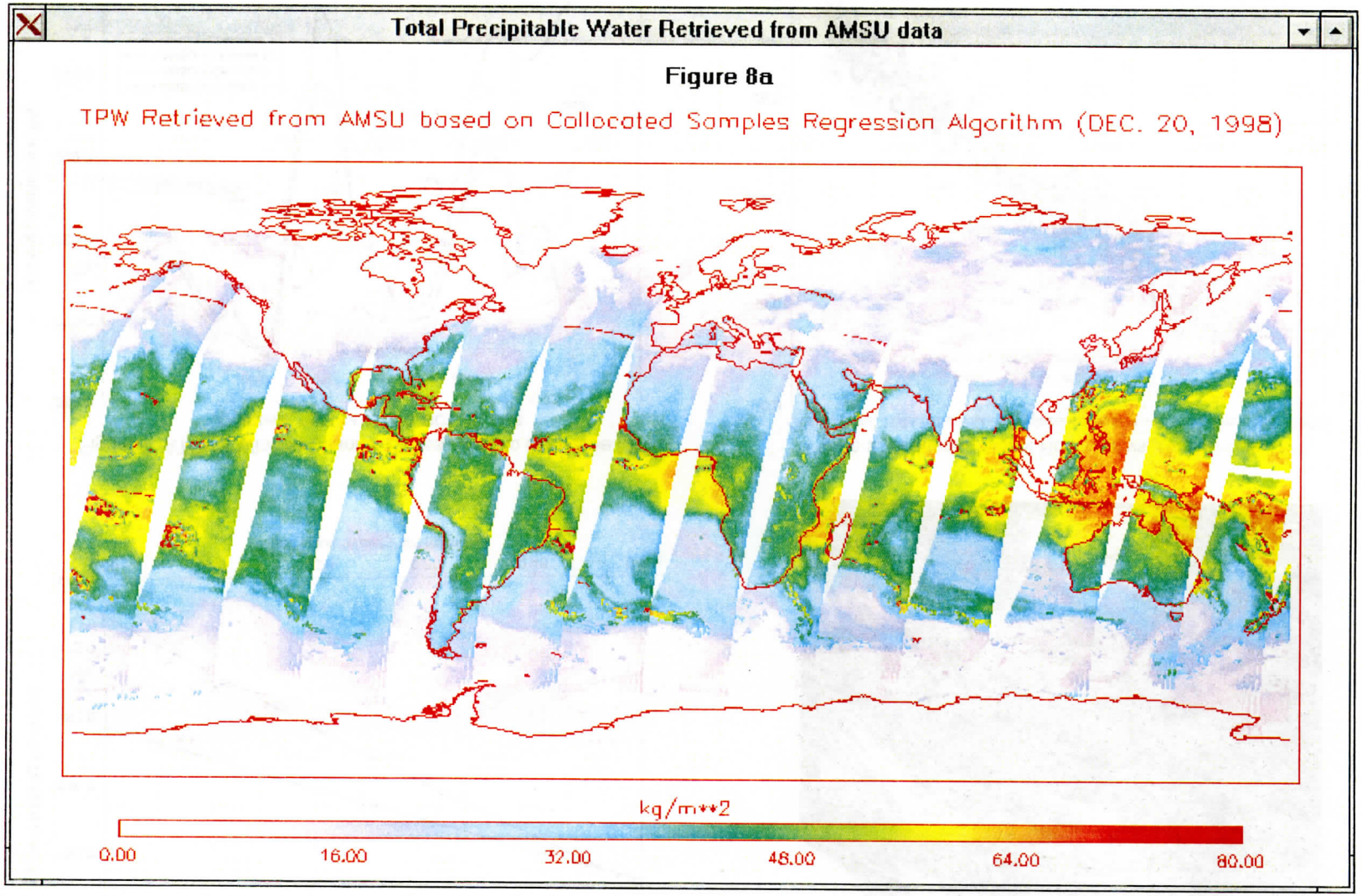
Total Precipitable Water Retrieved from AMSU data
Figure 8a
TPW Retrieved from AMSU based on Collocated Samples Regression Algorithm (DEC. 20, 1998)
kg/m**2
0.00
16.00
32.00
48.00
64.00
80.00

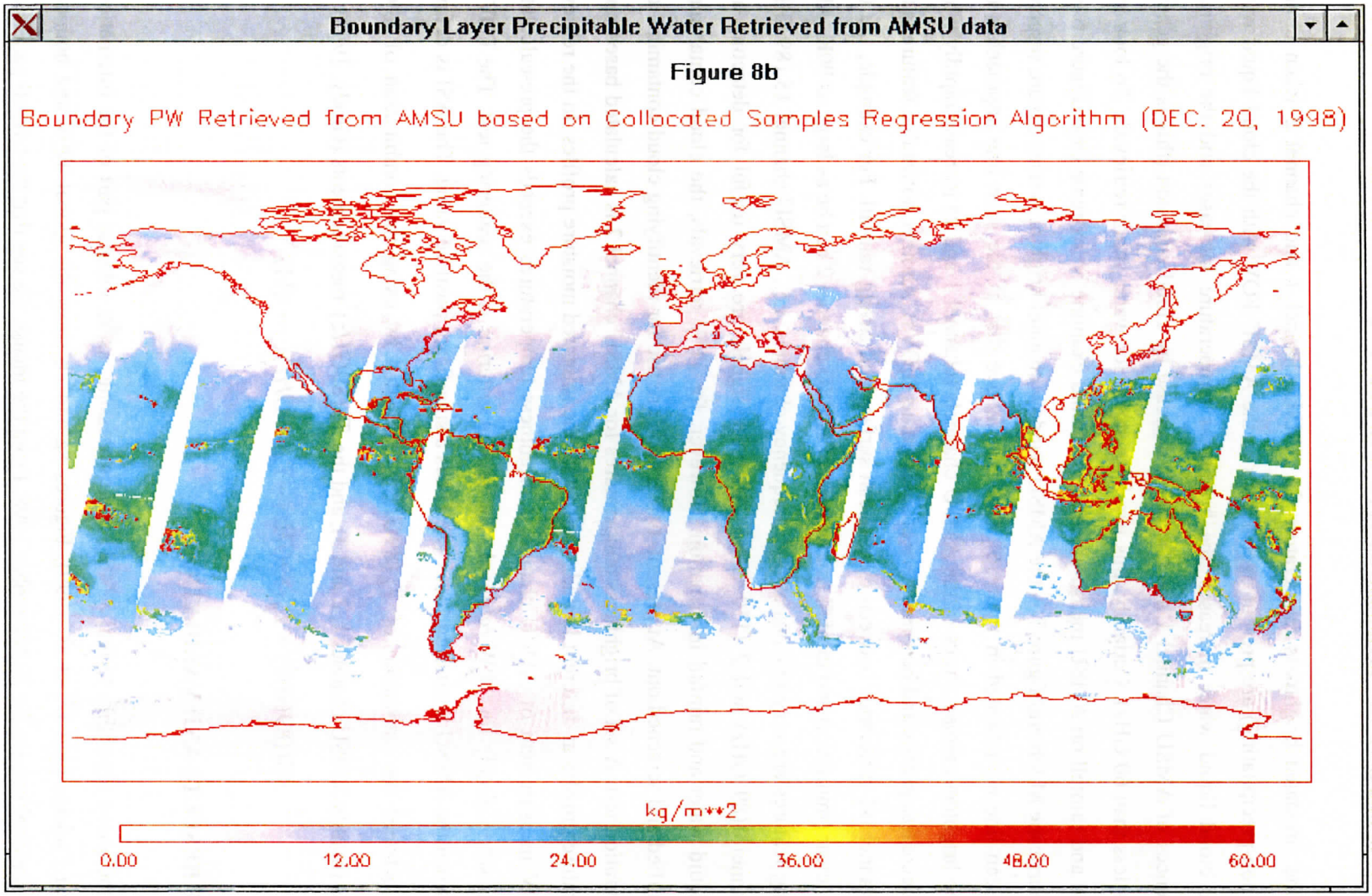
Boundary Layer Precipitable Water Retrieved from AMSU data
Figure 8b
Boundary PW Retrieved from AMSU based on Collocated Samples Regression Algorithm (DEC. 20, 1998)
kg/m**2
0.00
12.00
24.00
36.00
48.00
60.00

5. RAIN AND CLOUD EFFECT ON THE ALGORITHM ACCURACY

Figure 5 depicts the simulated brightness temperature for AMSU channel 1 and channel 2 when clouds (precipitating and non-precipitating) are present over oceans in the AMSU FOV with the cloud liquid water increasing. As the cloud liquid water increases, the brightness temperature increases and the brightness temperature differences of AMSU Channel 1 and channel 2 decrease by cloud emission (this is the general case at frequencies less than 60 GHz). Certainly, this is a false signal for water vapor retrievals. To look into the impact of cloud and rainfall on AMSU measurements, we should examine an extreme case. Figure 6 is a GOES picture of hurricane Mitch and figure 7 is the AMSU window channel brightness temperature response to the hurricane (scan line as indicated in figure 6). One may notice that as the scan line approaches the hurricane center the brightness temperatures of the AMSU channels (channel 1 and 2) increase rapidly while the BT difference decreases greatly and becomes zero at some points (FOVs). Another noticeable feature is the AMSU window channel BT difference between clear-ocean surface and strong rainfall. For example, the BT difference between clear (minimum) and rainfall (maximum) of AMSU channel 2 can be as large as 90K. Also the strong scattering features are very obvious at high frequency channels, i.e., AMSU channel 15 (89 GHz) and AMSU-B channel 1(89 GHz) and 2 (150 GHz). All these signals are very useful for detecting and retrieving cloud liquid water and rainfall information. However, for TPW retrievals, the cloud containment FOV must be identified and screened out. At present, two criteria are use for identifying cloud contamination. The first is the saturation test. A set of brightness temperatures for AMSU channel 2 is calculated based upon the climate temperature profiles at different latitude zones with the saturated moisture profiles. In the retrieval process, if the FOV measurement of AMSU channel 2 brightness temperatures exceeds the pre-calculated values; the FOV is set to cloudy for TPW retrieval. The second criterion is the scattering test. The FOV is flagged with rain when the AMSU Scattering Index (ASI) has a significant positive value. The ASI is defined as the difference between the estimation of $\hat{T}_B(89GHz)$, estimated by using the combination of lower frequency channels (mainly AMSU channel 1, 2 and 3), and the $T_B(89GHz)$ measurements (Grody, 1993):

$$ASI(89GHz) = \hat{T}_B(89GHz) - T_B(89GHz) \cdots\cdots (11)$$

6. ANALYSIS OF RESULTS AND VALIDATION

We have applied the above algorithm to real AMSU data processing, as an integral part of the International ATOVS Processing Package (Jun Li, et al, 1999). Figures 8a and 8b show the global TPW and boundary precipitable water retrieval images for 20 November 1998. From the image, we see that the overall patterns of the retrieval results are quite reasonable. A large value region is located between 30N - 30 S, exhibiting

variations along longitude and has a maximum region in the western Pacific Ocean. Over land, the retrieval results are also reasonable. For example, the high value regions are mainly located around the tropics and subtropics, as well as along the coast areas. High terrain areas, such as the Tibet Plateau of China and the Rocky Mountain region of the United States, are TPW minimum areas. This reasonable horizontal distribution makes the results useful for research and applications.

For quantitative validation of the retrieved TPW and boundary precipitable water, a one-month (December 1998) collocated data set was established as the validation data set. The criteria for selecting the collocations are the same as for the data set used for generating the regression coefficients. Figure 9 displays the validation results for TPW over ocean. In total, there are more than 1200 comparisons. The biases for TPW and BPW are quite small, 0.065 and -0.146, respectively. The RMS for TPW and BPW are 4.5 (mm) and 3.7 (mm), corresponding to RMS relative errors of 13.8% and 16.2%, respectively. The radiosonde errors are also included in the statistics. For validation over land, there are more than 5,000 comparisons, and the relative RMS is about 22%. This means that the TPW over land should (and could) be improved further by using AMSU-B measurements

7. CONCLUSION

The results and validations shown above are quite promising with almost no bias and reasonable RMS error for TPW. The TPW relative RMS error is less than 14%. Further improvements could be achieved if the AMSU-B measurements could be used.

REFERENCE

Grody, N. 1993: Remote sensing of the atmosphere from satellites using microwave radiometry, Atmospheric remote sensing from microwave radiometry, chapter 6, A wiley-interscience publication.

Kidder, S. Q. et al. 1995: Satellite Meteorology, Academic Press.

Li, J. 1994: Temperature and water vapor weighting functions from radiative transfer equation with surface emissivity and solar reflectivity. Advances in Atmospheric Sciences, Vol. 11, No. 4

Jun Li, et al, 1999: International ATOVS Processing Package (IAPP): The algorithm development and its application in real data processing, this proceeding

P. K. Rao, et al. 1994: Weather Satellites: system, data and environmental applications, American Meteorological Society.

Zeng Qingcun, 1974: Principle of atmospheric infrared remote sensing, Academic Press, p174.

TECHNICAL PROCEEDINGS OF THE TENTH INTERNATIONAL ATOVS STUDY CONFERENCE

Boulder, Colorado

27 January - 2 February 1999

Edited by

J. Le Marshall and J.D. Jasper

Bureau of Meteorology Research Centre, Melbourne, Australia

Published by

Bureau of Meteorology Research Centre

PO Box 1289K, GPO Melbourne, Vic., 3001, Australia

December 1999